Frontiers in Heat and Mass Transfer (FHMT), 19, 19 (2022)
DOI: 10.5098/hmt.19.19

Global Digital Central
ISSN: 2151-8629

Frontiers in Heat and Mass Transfer

Available at www.ThermalFluidsCentral.org

PREDICTING THE WAX DEPOSITION RATE BASED ON EXTREME LEARNING MACHINE

Qi Zhuang[a,*], Zhuo Chen[b], Dong Liu[c], Yangyang Tian[d]

[a] *The Second Gas Production Plant, PetroChina Changqing Oilfield Company, Xi'an China*
[b] *Sinopec Northwest Oil field Company, Urumqi, China*
[c] *Safety and Environmental Supervision Department, PetroChina Changqing Oilfield Company, Xi'an China*
[d] *Shaanxi Key Laboratory of Advanced Stimulation Technology for Oil & Gas Reservoirs, College of Petroleum Engineering, Xi'an Shiyou University, Xi'an China*

ABSTRACT

In order to improve the accuracy and efficiency of wax deposition rate prediction of waxy crude oil in pipeline transportation, A GRA-IPSO-ELM model was established to predict wax deposition rate. Using Grey Relational Analysis (GRA) to calculate the correlation degree between various factors and wax deposition rate, determine the input variables of the prediction model, and establish the Extreme Learning Machine (ELM) prediction model, improved particle swarm optimization (IPSO) is used to optimize the parameters of ELM model. Taking the experimental data of wax deposition in Huachi operation area as an example, the prediction performance of the model is evaluated by modeling and simulation, and compared with other models. The results show that the Mean Relative Error (MRE) and the Root Mean Square Error (RMSE) of the GRA-IPSO-ELM model are 0.351% and 0.049 respectively. Compared with other models, the GRA-IPSO-ELM model has better prediction performance.

Keywords: *Waxy crude oil, Wax deposition rate; Grey Relational Analysis (GRA); Improved Particle Swarm Optimization (IPSO); Extreme Learning Machine (ELM)*

1.INTRODUCTION

Crude oil pipeline transportation is the most commonly used crude oil transportation mode at present because of its advantages of large transportation capacity, economy, environmental protection and easy management. Most domestic crude oil has the characteristics of high pour point, high viscosity and high wax content. During the pipeline transportation of waxy crude oils, with the change of pipeline pressure and temperature conditions, heavy components such as wax, colloid and asphaltene in crude oils are easy to precipitate in solid form, and wax deposits are formed on the pipeline wall (Quan *et al*., 2015; Liu *et al*., 2021). Wax deposition will reduce the effective flow area of the pipeline, increase the flow resistance, reduce the transportation capacity, and even block the pipeline in severe cases, and the pig is prone to jam and other faults during pigging operation (Zhang *et al*., 2019). In order to reduce the wax deposition rate, different scholars theoretically clarify the wax deposition mechanism of multiphase waxy crude oil, a new high efficiency polymer pour point depressant for waxy crude oil was developed in practice (Li *et al*., 2021; Li *et al*., 2021). However, some wax is still deposited on the pipe wall, which still needs to be removed mechanically by pigging operation. In order to provide theoretical guidance for pipeline pigging, it is very important to establish wax deposition model to predict wax deposition in actual pipeline. According to different research emphases, wax deposition prediction models can be divided into thermodynamic model, kinetic model and computer training model. Among them, thermodynamic models mostly use the theory of phase equilibrium and phase transition to predict the wax precipitation point and wax precipitation from crude oil. Common thermodynamic models of wax deposition include regular solution model, polymer solution model and equation of state model. The wax deposition kinetics model is mostly based on Fick diffusion law. By analyzing the specific wax deposition mechanism and influencing factors in the pipeline transportation process, the wax deposition rate equation is established, and the parameters in the equation are determined by indoor simulation test, and finally the wax deposition kinetics model is obtained. There are many kinetic models about wax deposition at home and abroad, among which the representative models are Burger model, Hsu model, Hernandez model and Huang Qi-yu model. The computer training model trains and predicts wax deposition data through intelligent algorithm, and then obtains wax deposition rate.

In recent years, with the development of computer technology, various models based on neural network, particle swarm optimization and other intelligent algorithms to simulate training and then predict wax deposition have been applied and popularized (Su *et al*., 2016). Using this method, there is no need to explore the specific mechanism of wax deposition in detail. By adopting a suitable machine learning algorithm, based on the input original data, the relationship between simulated wax deposition rate and various influencing factors is trained, and then the wax deposition amount in other running states is determined, thus predicting the wax deposition situation. Zhou S. D. et al. took the lead in constructing Back Propagation (BP) Neural Networks, but only considered the effects of dynamic viscosity of crude oil, shear stress at pipe wall, temperature gradient at pipe wall and wax molecular concentration gradient at pipe wall on wax deposition rate, which proved the feasibility of this method (Zhou *et al*., 2004). On this basis, Tian Z et al. comprehensively considered the effects of oil temperature, wall temperature, dynamic viscosity of crude oil, shear stress at pipe wall, flow velocity, temperature gradient at pipe wall and concentration gradient of wax molecule at pipe wall on wax deposition rate, a 7-10-1 three-layer BPNN model is established to predict wax deposition rate

* Corresponding Author. E-mail: 1900679914@qq.com.

Global Digital Central
ISSN: 2151-8629

(Tian *et al*., 2014). However, due to the inherent defects of BPNN model, the prediction accuracy is relatively low. Xie and Xu established Radial Basis Function (RBF) Neural Network to predict wax deposition rate, and obtained that the relative error of this model is 1.5% (Xie and Xu, 2016). Wang et al. established a support vector machine model to predict wax deposition rate, which proved that this method is effective in predicting wax deposition (Wang *et al*., 2015). Zhang Y et al. by comparing the wax deposition rate predicted by RBF neural network and support vector machine, it is concluded that the prediction accuracy of support vector machine model is relatively high (Zhang *et al*., 2021). Xiao R. G. et al. optimized BP neural network through whale algorithm, which greatly improved the prediction accuracy of wax deposition rate (Xiao *et al*., 2022). The predictive values of the prediction models established in the above research are consistent with the real values, but the machine learning algorithms such as BP neural network and support vector machine, have the problems of large computation and low training efficiency under the condition of large samples.

Extreme learning machine is a single-layer feedforward neural network algorithm proposed by HUANG (Huang *et al*., 2006). It randomly selects the number of hidden layer nodes. Compared with the traditional machine learning method, this method has fast learning speed and strong generalization ability, but it also has some shortcomings. The weights and thresholds of randomly generated hidden layer nodes may lead to invalid hidden layer nodes, resulting in insufficient generalization ability and poor prediction effect (Zhao *et al*., 2022). Therefore, this paper proposes a wax deposition rate prediction model GRA-IPSO-ELM based on grey relational analysis (GRA), improved particle swarm optimization (IPSO) algorithm and extreme learning machine (ELM). Using GRA to calculate the correlation degree between various factors and wax deposition rate, and determine the input layer number of the model. IPSO algorithm is used to optimize the weight and threshold of ELM, and then the optimized model is used to predict wax deposition rate. Taking wax deposition experimental data in Huachi operation area as an example, the model is trained and simulated, and the prediction performance of the combined model is verified by index evaluation and model comparison.

2. THEORETICAL BASIS

2.1 Grey Relational Analysis (GRA)

Grey relational analysis method is a method to measure the degree of correlation between factors according to the similarity or dissimilarity of development trends among factors (Deng. 1990). It divides the relationships among multiple factors in complex systems by comparing the geometric relationships among statistical sets. The specific steps are as follows:

(1) Determine the reference sequence and the comparison sequence

Reference series refers to the data series that reflect the behavior characteristics of the system, while comparison series refers to the data series composed of factors that affect the behavior of the system. The sequence of wax deposition rate is taken as reference sequence Y_0, and the sequence of other influencing factors is comparative sequence X_i (i takes 1 ~ m), as shown in Formula 1.

$$\begin{aligned} Y_0 &= (Y_0(1), Y_0(2), \cdots, Y_0(n)) \\ X_i &= (X_i(1), X_i(2), \cdots X_i(n)) \end{aligned} \tag{1}$$

(2) Dimensionless

In order to eliminate the influence of different units of data on the results, the reference series and comparison series are dimensionless. Among them, dimensionless includes mean value method, initial value method, etc. This time, the initial value method is used for dimensionless treatment, as shown in Formula 2.

$$Y_0^{'} = \frac{Y_0}{Y_0(1)}, X_i^{'} = \frac{X_i}{X_i(1)} \tag{2}$$

(3) Calculate grey correlation coefficient

The difference sequence Δi(k), two-order minimum m, two-order maximum M and correlation coefficient γ are calculated respectively according to Formula 3~6.

$$\Delta_i(\mathrm{k}) = \left| Y_0^{'}(\mathrm{k}) - X_i^{'}(\mathrm{k}) \right| \tag{3}$$

$$m = \min_i \min_k \Delta_i(k) \tag{4}$$

$$M = \max_i \max_k \Delta_i(k) \tag{5}$$

$$\gamma(Y_0^{'}, X_i^{'}) = \frac{m + \rho M}{\Delta_i(k) + \rho M} \tag{6}$$

Where: ρ is the resolution coefficient, and the value range is (0, 1), usually 0.5.

(4) Calculate grey relational degree

The correlation degree is the average of the above grey correlation coefficients, as in Formula 7.

$$\gamma(\mathrm{Y}_0, \mathrm{X}_i) = \frac{1}{N} \sum_{k=1}^{N} \gamma(Y_0^{'}, X_i^{'}) \tag{7}$$

2.2 Extreme Learning Machine (ELM)

Extreme Learning Machine (ELM) is a machine learning method developed on the basis of feedforward neural network. The model consists of three layers, namely input layer, hidden layer and output layer. The network structure of ELM model is shown in Figure 1. In the training and fitting process, the ELM model will randomly generate the connection weights between the input layer and the hidden layer and the threshold of the hidden layer neurons, and the unique optimal solution can be obtained only by defining the number of hidden layer neurons without adding subjective will. Compared with the traditional neural network, this model has the advantages of strong generalization ability, fast training speed and simple parameter setting, etc. At present, it has been widely used in many fields and achieved good results.

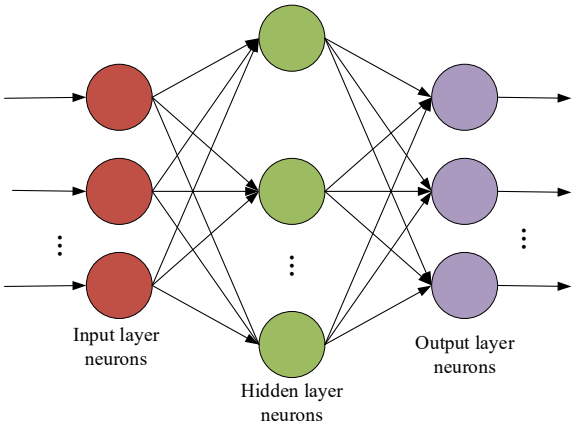

Fig. 1 Network structure of extreme learning machine

For the prediction of wax deposition rate, it is assumed that there are N arbitrary samples (X_i, Y_i), where:

$$\begin{aligned} X_i &= [x_{i1}, x_{i2}, x_{i3}, \cdots, x_{in}]^T \in R^n; \\ Y_i &= [y_{i1}, y_{i2}, y_{i3}, \cdots, y_{in}]^T \in R^m \end{aligned} \tag{8}$$

Then the output of the single hidden layer feedforward neural network is:

$$\sum_{i=1}^{K} \beta_i g(W_i \cdot X_i + B_i) = t_i \tag{9}$$

Where: K represents the number of nodes set by the hidden layer, $g(x)$ is the excitation function of hidden layer, $W_i=[w_{i,1},w_{i,2},w_{i,3},\cdots,w_{i,n}]^T$ is the connection weight vector between the input layer and the hidden layer, $\beta_i=[\beta_{i,1}, \beta_{i,2}, \beta_{i,3},\cdots, \beta_{i,n}]^T$ is the connection weight vector between

the output layer and the hidden layer, B_i is the offset value of the i-th node in the hidden layer neuron nodes, $W_i \cdot X_j$ represents the inner product of W_i and X_j.

Single-layer neural network learning minimizes the output error by approaching the zero error of sample N, which can be expressed as:

$$\sum_{i=1}^{N} \left\| t_i - Y_i \right\| = 0 \tag{10}$$

That is, there are β_i, W_i and B_i, so that:

$$\sum_{i=1}^{K} \beta_i g(W_i \cdot X_i + B_i) = Y_i \tag{11}$$

Formula 11 can be expressed by a matrix as $H\beta=T$. Where, H is the output matrix of the hidden layer, β is the output weight, and T is the expected output. When the hidden layer excitation function $g(x)$ selected in the model is infinitely differentiable, the input weight w and hidden layer bias B can be initialized randomly, and the output weight β can be obtained by the Formula 12.

$$\beta = H^{+}T \tag{12}$$

Where, H^{+} is the generalized inverse of Moore-Penrose of matrix H.

2.3 Particle Swarm Optimization (PSO)

Particle swarm optimization (PSO) is an optimization algorithm proposed by KENNEDY et al. in 1995(Kennedy and Eberhart. 1995). The core idea of this algorithm comes from the study of bird predation behavior. After continuous exploration and improvement in the later period, it has become a very important part in the field of intelligent algorithms. Each particle represents a possible solution vector. The quality of the particle is judged according to the fitness function value. By learning from the global and individual optimal solutions, the particle position and speed are continuously updated, and finally the purpose of global optimization is realized.

Assuming that there is a particle population of size n in the D-dimensional search space, the position and velocity of each particle are updated according to the following formula:

$$V_{id}(t+1) = wV_{id}(t) + c_1 r_1 (P_{id}(t) - X_{id}(t)) + c_2 r_2 (P_{gd}(t) - X_{id}(t)) \tag{13}$$

$$X_{id}(t+1) = X_{id}(t) + V_{id}(t+1) \tag{14}$$

Where: t is the number of iterations, $P_{id}(t)$ is the individual optimal solution of the particle for the t-th iteration, $P_{gd}(t)$ is the global optimal solution of the particle for the t-th iteration, w is inertia weight, c_1 and c_2 are learning factors, r_1 and r_2 are uniformly distributed random numbers between [0 1].

2.4 Improved Particle Swarm Optimization (IPSO)

Aiming at the shortcomings of standard particle swarm optimization algorithm in high-dimensional multi-objective function, such as easy to fall into local optimal trap, low search accuracy and easy to cause premature phenomenon (Chen and Zou. 2022), an improved optimized particle swarm optimization algorithm is proposed.

Firstly, asynchronous learning factor is introduced. The researchshows that giving a large value of C_1 and a small value of C_2 at the initial iteration of standard particle swarm optimization can make the "population" tend to learn by itself, which is beneficial to improve the global search ability of the algorithm; In the later iteration process, keeping C_1 decreasing linearly and C_2 increasing linearly can effectively avoid the population individual falling into the local optimal range and greatly improve the convergence speed of the algorithm(Teng *et al*., 2017). In this paper, asynchronous learning factor is introduced and defined as follows:

$$C_1 = C_{start1} + (C_{cend1} - C_{start1}) \frac{t}{T} \tag{15}$$

$$C_2 = C_{start2} + (C_{cend2} - C_{start2}) \frac{t}{T} \tag{16}$$

Where: C_{start1} and C_{cend1} represent the initial and final values of self-learning factors, which are taken as 2.5 and 0.75 respectively in this paper, C_{start2} and C_{cend2} represent the initial and final values of social learning factors, which are taken as 0.5 and 2.25 respectively in this paper, T is the maximum number of iterations; t is the current number of iterations.

Adaptive inertia weight is introduced. In the standard particle swarm optimization algorithm, because the inertia weight affects the current velocity, the constant inertia weight is not conducive to the optimization ability of particle swarm optimization, and may lead to the local optimal trap in the process of particle search, which may lead to premature convergence. Excessive inertia weight is beneficial to improve the global search ability of the algorithm; However, when the inertia weight is small, it is beneficial to improve the local search ability of the algorithm.

In this paper, the new inertia weight of nonlinear change is used for reference proposed by Chen (Chen and Zou. 2022). The scheme has a good balance between global search ability and local search ability. The larger inertia coefficient in the early stage is beneficial to search the global optimal solution, the turning transformation of inertia coefficient in the middle stage expands the search range, and the smaller inertia coefficient in the later stage is beneficial to search the local optimal solution. The inertia weight is updated according to the following formula.

$$w = 2 \times \left(-\frac{w_{\max} - w_{\min}}{T} t\right) + \frac{w_{\max} - w_{\min}}{1.0 + e^{-(\frac{12}{T}t-6)}} + w_{\max} \tag{17}$$

Where: w_{max} is the maximum inertia weight, which is 0.8 in this paper, w_{min} is the minimum inertia weight, and this paper takes 0, T is the maximum number of iterations; t is the current number of iterations.

3. MODEL BUILDING AND VALIDATION

3.1 Model Building Process

Because the number of input nodes in the ELM model will affect the complexity of the network structure, the input weights and hidden layer thresholds are randomly generated, which will lead to the instability of the ELM network performance and the inability to guarantee the prediction accuracy. In order to solve the above problems, grey relational analysis is used to calculate the relational degree between various factors and wax deposition rate, and the number of input layers of ELM model is determined. The IPSO algorithm was used to optimize the initial weights and thresholds of the ELM model, and IPSO-ELM models for predicting wax deposition rate of waxy crude oil are constructed. The specific model construction process is shown in Figure 2.

The steps of improving particle swarm optimization (IPSO) algorithm to optimize extreme learning machine are as follows:

Step1: Establish a data set according to the wax deposition experimental data in Huachi operation area, randomly sample 80% of the data set data as the training set of IPSO algorithm to optimize ELM model, and the remaining 20% as the test set of IPSO algorithm to optimize ELM model;

Step2: Given the initial parameters of the improved particle swarm optimization, the iteration times, the population size, the specified position and velocity constraint range, the problem dimension, the adaptive inertia weight value range, and the initial and final values of the learning factor;

Step3: Random initial particle position and velocity, calculate the fitness value of each particle according to the objective function, and initialize the individual optimal value and global optimal value of population particles;

Step4: Using the optimized velocity and position update formula, the particle velocity and position are updated through iterative optimization;

Step5: Judge the constraint conditions and calculate the fitness of each individual position of the new population, calculate the individual optimal value obtained each time through iterative updating of the position, compare with the historical individual optimal value, select the optimal value as the individual optimal value, update it to the global optimal solution, and update the global optimal value asynchronously with the continuous iteration of particles;

Step6: Judge whether the algorithm termination condition is met through the given maximum iteration times constraint. If the termination condition is not met, go to Step4 to continue execution, and calculate the global optimal solution within the specified iteration times.

3.2 Model Validation Indicators

In order to verify the prediction effect of the model, the Mean Relative Error (MRE), Root Mean Square Error (RMSE) and Coefficient of determination (R^2) are selected as evaluation indexes. Among them, the smaller the MRE, the smaller the RMSE and the larger the R^2, the higher the fitting degree of the model. The specific calculation formula is shown in Formula 17-19 (Ling *et al*., 2021).

$$MRE = 100 \times \frac{1}{N} \sum_{i=1}^{N} \frac{\left| y_i - \hat{y}_i \right|}{y_i} \tag{17}$$

$$RMSE = \sqrt{\frac{1}{N} \sum_{i=1}^{N} (y_i - \hat{y}_i)^2} \tag{18}$$

$$R^2 = \frac{\left(N \sum_{i=1}^{N} y_i \hat{y}_i - \sum_{i=1}^{N} y_i \sum_{i=1}^{N} \hat{y}_i \right)^2}{\left[N \sum_{i=1}^{N} (\hat{y}_i)^2 - (\sum_{i=1}^{N} \hat{y}_i)^2 \right] \left[N \sum_{i=1}^{N} y_i - (\sum_{i=1}^{N} y_i)^2 \right]} \tag{19}$$

Where: y_i is the actual value of wax deposition rate, $\hat{y}_i$ is the predicted value of wax deposition rate, N is the total number of test samples.

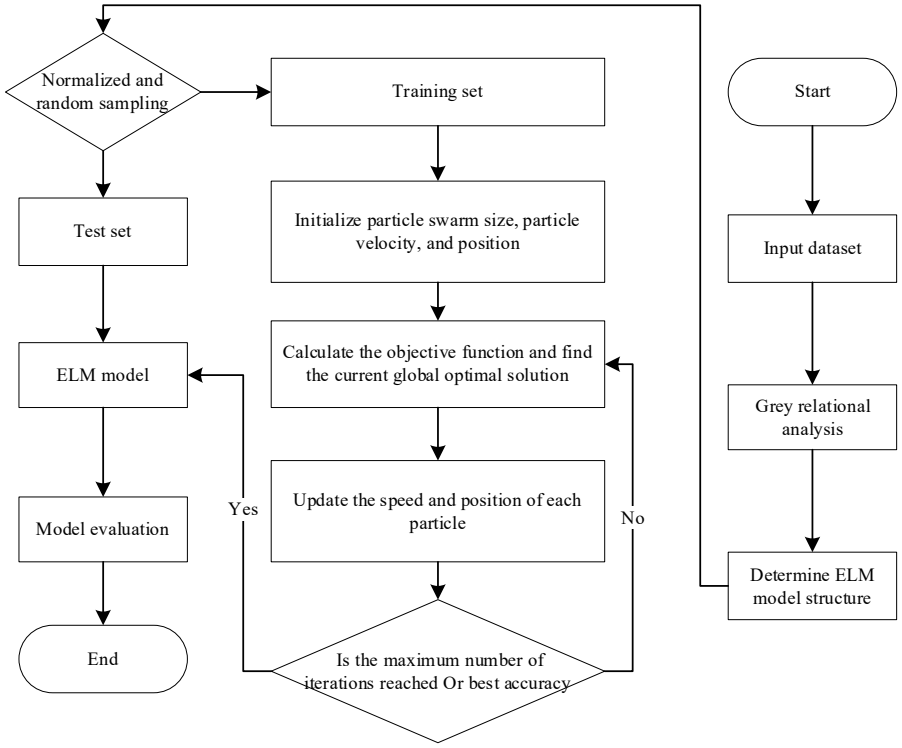

Fig. 2 IPSO-ELM algorithm flow

4. EXAMPLE APPLICATION

4.1 Data preparation

There are many factors affecting wax deposition rate, and there is a very complex nonlinear relationship among these factors. Through the wax deposition experiment in Huachi operation area, the wax deposition rate X_8 under different oil temperature X_1, wall temperature X_2, crude oil viscosity X_3, shear stress at pipe wall X_4, flow velocity X_5, temperature gradient at pipe wall X_6 and wax molecular concentration gradient at pipe wall X_7 was obtained. The specific wax deposition experimental data are shown in Table 1 (Wang. 2010). In the training process of sample data, the dimensions of input variables and output variables are not the same, it is necessary to normalize the sample data before training. The variables are converted to numbers between [0, 1] by Formula 20.

$$x_i^* = \frac{x_i - \min}{\max - \min} \tag{20}$$

Where: x_i^* represents the sample data after processing, x_i represents the data before processing.

4.2 Grey Relational Analysis and Processing

Using the grey relational analysis method, the grey relational analysis of each influencing factor is carried out, and the relational degree between each influencing factor and wax deposition rate is shown in Table 2. It can be seen from Table 2 that various influencing factors have different influences on wax deposition rate. The relational degree is

Global Digital Central
ISSN: 2151-8629

arranged in order of size, and the results are as follows: crude oil viscosity > wax molecular concentration gradient at pipe wall > oil temperature > wall temperature > shear stress at pipe wall > temperature gradient at pipe wall > flow velocity. In this paper, the relational degree of 7 factors to wax deposition rate is greater than 0.6945. Except for 4 factors (shear stress at pipe wall, temperature gradient at pipe wall, wax crystal solubility coefficient at pipe wall and crude oil viscosity), the other 3 factors (wall temperature, oil temperature and flow velocity) can not be ignored. Therefore, the seven factors should be used as the input of ELM model, that is, the number of input layers of ELM model is 7.

Table 2 Grey relational degree between each influencing factor and wax deposition rate

Variable	Grey relational degree
X_1	0.7663
X_2	0.7622
X_3	0.8655
X_4	0.7537
X_5	0.6945
X_6	0.6946
X_7	0.8101

4.3 Result Analysis and Model Comparison

Randomly select training set and test set from 38 groups of original data, among which 30 groups of training set data and 8 groups of test set data are substituted into ELM model for training according to the steps set above. The number of hidden layer nodes is optimized by trial-and-error method. When the initial number of hidden layer nodes is 30, the mean square error of the model is the smallest. Therefore, the number of nodes in the hidden layer of the extreme learning machine is determined to be 30, and the network structure of the extreme learning machine is determined to be 7-30-1.

In order to compare the effectiveness and efficiency of each algorithm model, ELM, PSO-ELM and IPSO-ELM algorithm models are selected for comparison. In this example, the mathematical models are solved and analyzed by Matlab 2020a software under the conditions of AMD Ryzen 7 4800U CPU @ 1.80 GHz, memory 16.0 GB and windows 10 operating system. Among them, the parameters of PSO algorithm are set as follows: the maximum iteration times is 150 times, the population size is 30; learning factors C_1 and C_2 are all 1.5. The learning factor C_1 of IPSO is calculated by Formula 15, the learning factor C2 of IPSO is calculated by Formula 16; The inertia weight W of IPSO is calculated by Formula 17, and other parameters are unchanged. The mean square error of each iteration is recorded and compared by drawing. As can be seen from Figure 3, compared with PSO-ELM model, IPSO-ELM model has more ideal optimization effect.

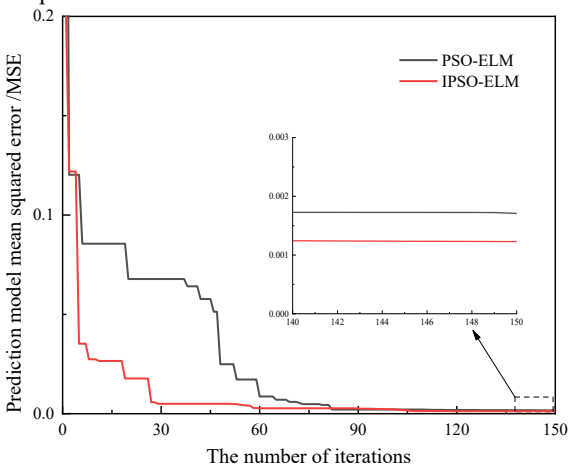

Fig. 3 Iterating 150 times for different models

In order to test the prediction accuracy of IPSO-ELM model, GA-ELM, PSO-ELM and ELM are selected to compare with them. The results are shown in Figure 4 and Table 3. As can be seen from Figure 4, compared with ELM model, the difference between the predicted values and the actual values of GA-ELM, PSO-ELM and IPSO-ELM models is smaller, and the fitting effect is better. The mean relative error (MRE) of ELM, GA-ELM, PSO-ELM and IPSO-ELM are 5.164%, 3.765%, 0.544% and 0.351%, respectively. The MRE of IPSO-ELM are lower than those of other models, indicating that the prediction accuracy of this model is the highest.

In order to evaluate the prediction performance of the model, the three statistical indicators mentioned above are used to evaluate the model, and the analysis results are shown in Table 4. From the mean relative error (MRE) index, IPSO-ELM decreased by 3.414%, 0.193% and 4.813% compared with GA-ELM, PSO-ELM and ELM respectively. From the Root Mean Square Error (RMSE), IPSO-ELM decreased by 0.425, 0.008 and 0.842 compared with GA-ELM, PSO-ELM and ELM, respectively. And the determination coefficient (R^2) of IPSO-ELM is 0.99985, which is closest to 1, indicating that the fitting degree of IPSO-ELM model is high and the prediction effect is good.

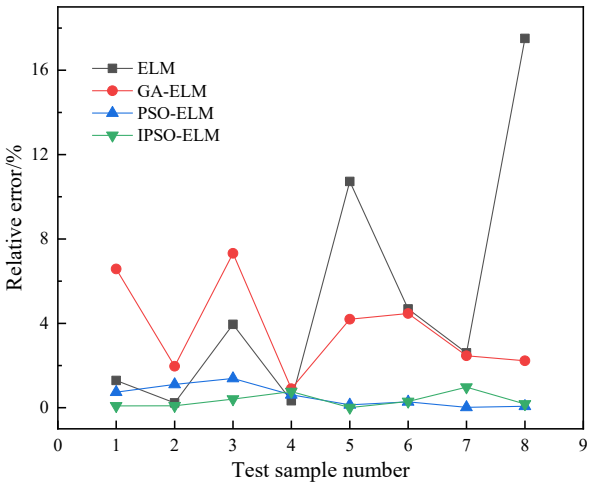

Fig. 4 Comparison of relative errors

Table 4 Comparison of model performance indicators

Model	MRE/%	RMSE	R^2
ELM	5.164	0.891	0.96444
GA-ELM	3.765	0.474	0.98940
PSO-ELM	0.544	0.057	0.99976
IPSO-ELM	0.351	0.049	0.99985

In order to further explore the stability of PSO and IPSO optimized ELM models, PSO-ELM model and IPSO-ELM model were used to predict wax deposition rate for 10 times, and the Mean Relative Error of each prediction result is shown in Table 5. It can be seen from Table 5 that in the 10 prediction results, the Mean Relative Error varies in different degrees, and there is no obvious law. The Mean Relative Error of PSO-ELM model is approximately in the range of 0.5% ~ 0.6%, while that of IPSO-ELM model is approximately in the range of 0.2% ~ 0.4%, which indicates that PSO and IPSO optimized ELM model have good stability.

Table 5 The Mean Relative Error of the 10 prediction results

Time	PSO-ELM/%	IPSO-ELM/%	Time	PSO-ELM/%	IPSO-ELM/%
1	0.620	0.119	6	0.506	0.188
2	0.506	0.352	7	0.544	0.381
3	0.544	0.318	8	0.650	0.119
4	0.650	0.429	9	0.514	0.352
5	0.620	0.354	10	0.521	0.318

5. CONCLUSIONS

1) By using the grey relational analysis method, it is proved that the seven factors mentioned in this paper all have important influence on wax deposition rate. Therefore, when applying ELM model to predict wax deposition rate, it should be used as training dimension to predict wax deposition rate.

2) Through training and forecasting the wax deposition experimental data in Huachi operation area, the Mean Relative Error (MRE) and Root Mean Square Error (RMSE) of GRA-PSO-ELM model for predicting wax deposition rate are 0.351% and 0.049, which proves that GRA-IPSO-ELM model has high reliability and good prediction performance, and can provide decision support for the flow guarantee of waxy crude oil in pipeline transportation.

3) Using PSO-ELM model and IPSO-ELM to predict wax deposition rate for 10 times, the Mean Relative Error of PSO-ELM model to predict wax deposition rate is roughly in the range of 0.5% ~ 0.6%, the Mean Relative Error of IPSO-ELM model is roughly in the range of 0.2% ~ 0.4%, indicating that PSO-ELM and IPSO-ELM models have good stability.

Table 1 Experimental results of crude oil wax deposition rate in Huachi operation area

number	X_1 */℃*	X_2 */℃*	X_3 */(mPa.s)*	X_4 */Pa*	X_5 */(m.s^{-1})*	X_6 */(℃.mm^{-1})*	X_7 */(10^{-3}·℃$^{-1}$)*	X_8 */(g·m^{-2}·h^{-1})*
1	33	30	29.31	5.69	0.29	2.24	2.62	11.90
2	35	32	25.84	1.51	0.09	1.23	2.10	11.63
3	35	32	25.66	2.5	0.15	1.64	2.10	10.91
4	35	32	25.49	4.96	0.29	2.24	2.10	10.13
5	35	32	25.40	7.42	0.44	2.6	2.10	9.75
6	35	32	25.35	9.87	0.58	2.87	2.10	9.50
7	35	32	25.3	14.78	0.88	3.23	2.10	9.19
8	37	34	22.34	4.36	0.29	2.24	1.52	7.51
9	38	35	20.97	4.1	0.29	2.24	1.16	6.54
10	40	37	18.79	1.1	0.09	1.23	0.63	6.40
11	40	37	18.67	1.83	0.15	1.64	0.63	6.00
12	40	37	18.56	3.64	0.29	2.24	0.63	5.57
13	40	37	18.51	5.44	0.44	2.60	0.63	5.36
14	40	37	18.48	7.24	0.59	2.87	0.63	5.22
15	40	37	18.44	10.84	0.88	3.23	0.63	5.05
16	44	41	14.81	2.91	0.30	2.24	0.34	6.20
17	45	42	14.04	2.76	0.30	2.24	0.34	6.77
18	46	43	13.33	2.63	0.30	2.24	0.37	7.20
19	48	45	12.05	2.38	0.30	2.24	0.46	7.11
20	49	46	11.47	2.27	0.30	2.24	0.52	5.95
21	35	30	25.72	5.01	0.29	3.72	2.62	15.96
22	37	32	23.03	1.35	0.09	2.08	2.10	14.42
23	37	32	22.77	2.22	0.15	2.75	2.10	13.54
24	37	32	22.53	4.40	0.29	3.72	2.10	12.59
25	37	32	22.41	6.56	0.44	4.33	2.10	12.11
26	37	32	22.35	8.72	0.59	4.76	2.10	11.81
27	37	32	22.28	13.04	0.88	5.35	2.10	11.42
28	40	35	18.71	3.66	0.29	3.72	0.88	9.60
29	42	37	16.98	1.00	0.09	2.08	0.51	9.92
30	42	37	16.82	1.65	0.15	2.75	0.51	9.31
31	42	37	16.66	3.27	0.29	3.72	0.51	8.66
32	42	37	16.58	4.88	0.44	4.33	0.51	8.33
33	42	37	16.54	6.49	0.59	4.76	0.51	8.12
34	42	37	16.50	9.71	0.88	5.35	0.51	7.86
35	37	30	22.72	4.43	0.29	4.73	2.62	18.09
36	42	35	16.78	3.29	0.29	7.44	0.77	11.30
37	40	30	19.09	3.74	0.29	7.44	1.93	22.46
38	45	35	14.39	2.83	0.30	7.44	0.64	16.43

Table 3 Analysis of relative error results

number	*Experimental value*	*ELM*		*GA-ELM*		*PSO-ELM*		*IPSO-ELM*	
		Predictive value /(g·m^{-2}·h^{-1})	*Relative error/%*	*Predictive value /(g·m^{-2}·h^{-1})*	*Relative error/%*	*Predictive value /(g·m^{-2}·h^{-1})*	*Relative error/%*	*Predictive value /(g·m^{-2}·h^{-1})*	*Relative error/%*
2	11.63	11.780	1.290	10.865	6.578	11.716	0.739	11.640	0.086
8	7.51	7.527	0.228	7.362	1.968	7.427	1.107	7.517	0.093
9	6.54	6.281	3.954	6.061	7.321	6.631	1.388	6.513	0.407
13	5.36	5.378	0.330	5.408	0.899	5.393	0.614	5.401	0.765
21	15.96	14.248	10.727	16.630	4.198	15.938	0.138	15.950	0.006
23	13.54	12.906	4.682	14.145	4.468	13.578	0.281	13.580	0.295
24	12.59	12.263	2.597	12.900	2.462	12.588	0.016	12.710	0.977
28	9.60	7.919	17.507	9.386	2.228	9.593	0.071	9.583	0.176

NOMENCLATURE

X_1—Oil temperature, /℃
X_2—Wall temperature, /℃
X_3—Dynamic viscosity, /(mPa.s)
X_4—Shear stress at pipe wall, /Pa
X_5—Flow velocity, /(m.s^{-1})
X_6—Temperature gradient at pipe wall, /(℃.mm^{-1})
X_7—Wax molecular concentration gradient at pipe wall, /(10^{-3}·℃$^{-1}$)
X_8—Wax deposition rate, /(g·m^{-2}·h^{-1})

REFERENCES

Chen, B.W. and Zou H. (2022). Self-Conclusion and Self-Adaptive variation Particle swarm optimization. Computer Engineering and Applications,58(08):67-75.
https://kns.cnki.net/kcms/detail/11.2127.TP.20210611.0933.002.html

Deng, J.L. (1990). Tutorial on grey system theory.

Huang, G. B., Zhu, Q. Y., Mao, K. Z., Siew, C. K., Saratchandran, P. and Sundararajan, N. (2006). Can threshold networks be trained directly?. *IEEE Transactions on Circuits and Systems II: Express Briefs*,*53*(3),187-191.
https://doi.org/10.1109/TCSII.2005.857540

Kennedy, J. and Eberhart, R. (1995). Particle Swarm Optimization. Icnn95-international Conference on Neural Networks.

Li, Q.B., Cao, J.C., Liu, Y., Cheng, Q.L and Liu, C. (2021). Effect of dispersed water on the paraffin crystallization and deposition of emulsified waxy crude oil via dissipative particle dynamics, Journal of Molecular Liquids, Volume 343:117679.
https://doi.org/10.1016/j.molliq.2021.117679

Li, Q.B., Deng, X.X, Liu, Y., Cheng, Q.L and Liu, C. (2021). Gelation of waxy crude oil system with ethylene-vinyl acetate on solid surface: A molecular dynamics study, Journal of Molecular Liquids, Volume 331:115816.
https://doi.org/10.1016/j.molliq.2021.115816

Ling, X., L.S. Xu, J.C. Gao, J.J. Ma, H.Q. Ma and X.H. Fu. (2021). Prediction of External Corrosion Rate of Oil Pipeline Based on Improved IFA-BPNN. Surface Technology, 50(04),285-293.
https://doi.org/10.16490/j.cnki.issn.1001-3660.2021.04.029

Liu, C.Y., S.Z. Luan, W.C. Han, X.Q. Zhang, X.L. Wang, Z.R. Li, J. Du and Z.Y. Guan. (2021). Comparison test on factors affecting wax deposition of waxy crude oil. Oil & Gas Storage and Transportation,40(01),78-83.
https://kns.cnki.net/kcms/detail/13.1093.TE.20201202.1537.004.html

Quan, Q., G. Jing, W. Wei and G. Ge. (2015). Study on the aging and critical carbon number of wax deposition with temperature for crude oils. Journal of Electronic Materials,130,1-5.
https://doi.org/10.1016/j.petrol.2015.03.026

Su, W.K., Q. L. Cheng and W. Sun. (2016). Progress in researching wax deposition model of oil pipelines. Chemical Engineering & Machinery,43(01),20-23.
https://doi.org/10.3969/j.issn.0254-6094.2016.01.005

Teng, Z.J., J. L. Lv, L.W. Guo, Z.X. Wang, H. Xu and L.H. Yuan. (2017). Research on particle swarm optimization algorithm based on dynamic acceleration coefficients. Microelectronics & Computer,34(12),125-129.
https://doi.org/10.19304/j.cnki.issn1000-7180.2017.12.026

Tian, Z., W.B. Jin, L. Zhou, Y.P. An and H.F. Wu. (2014). Prediction of wax deposition rate in pipeline by BP neural network. Journal of Xi'an Shiyou University(Natural Science Edition),29(01),66-70.
https://doi.org/10.3969/j.issn.1673-064X.2014.01.013

Wang, X.L. (2010). Prediction and analysis of wax deposition in pipeline crude oil in Huachi operation area. Xi'an Shiyou University.
https://doi.org/10.7666/d.y1854507

Wang, L., Z. Tian, H.T. Pu, W.B. Jin and L. Dong. (2015). Study of wax deposition rate prediction model based on support vector machines. Applied Chemical Industry, S1, 73-77.
https://kns.cnki.net/kcms/detail/detail.aspx?FileName=SXHG2015S1021&DbName=CJFQPREP

Xie, Y. and Yu, X. (2016). A prediction method for the wax deposition rate based on a radial basis function neural network. Petroleum,3(2),237-241.
https://doi.org/10.1016/j.petlm.2016.08.003

Xiao, R.G., Zhuang, Q., Jin, S.S and Jin, W.B. (2022). PREDICTION MODEL OF WAX DEPOSITION RATE BASED ON WOA-BPNN ALGORITHM. Frontiers in Heat and Mass Transfer (FHMT), 18–8.
https://doi.org/10.5098/hmt.18.8

Yu, Z., Y.W. Ruo and W. Xue. (2021). Prediction Method of Wax Deposition Rate in Crude Oil Pipeline Based on RBF Neural Network and Support Vector Machine. E3S Web of Conferences,271.
https://doi.org/10.1051/E3SCONF/202127104007

Zhang, S.M., Z.C. He, X.X. Zhu and N. Lu. (2019). Study on a new type of wax removal pig for crude oil pipeline. China Petroleum Machinery,47(02),136-144.
https://doi.org/10.16082/j.cnki.issn.1001-4578.2019.02.021

Zhao, Y.K., J. Hu and B. Yang. (2022). Slope stability analysis based on IPSO-ELM. Nonferrous Metals Engineering,12(01),122-128. https://doi.org/10.3969/j.issn.2095-1744.2022.01.018

Zhou, S.D., M. Wu and J. Wang. (2004). Wax deposition rate model for crude oil pipeline based on neural network. Journal of Xi'an Shiyou University(Natural Science Edition),19(01),38-40. https://doi.org/10.3969/j.issn.1673-064X.2004.01.009